Supporting informations for
# TeraHertz HgTe nanocrystals: beyond confinement

Nicolas Goubet[1,2,3], Amardeep Jagtap[1], Clément Livache[1,2,3], Bertille Martinez[1,2,3], Hervé Portalès[4], Xiang Zhen Xu[2,3], Ricardo P.S.M. Lobo[2,3], Benoit Dubertret[2,3], Emmanuel Lhuillier[1*]

[1]Sorbonne Université, CNRS, Institut des NanoSciences de Paris, INSP, F-75005 Paris, France
[2] LPEM, ESPCI Paris, PSL University, CNRS, F-75005 Paris, France
3 Sorbonne Université, CNRS, LPEM, F-75005 Paris, France
[4] Sorbonne Université, CNRS, De la Molécule aux Nano-objets: Réactivité, Interactions et Spectroscopies, MONARIS, F-75005 Paris, France

To whom correspondence should be sent : el@insp.upmc.fr

## Content

## 1. CHEMISTRY

### 1.1. Chemical compounds

Tellurium powder (Sigma-Aldrich, 99.99%), mercury chloride (Strem Chemicals, 99%), mercury bromide (Strem Chemicals), mercury iodide (Strem Chemicals, 99%), sodium borohydride (Sigma-Aldrich, 98%), Se powder (Sigma-Aldrich, 99,99%), sulfur powder (Sigma Aldrich, 99,99%), Trioctylphosphine (TOP, Cytek, 90%), dodecanthiol (DDT, Sigma Aldrich), oleic acid (Sigma-Aldrich, 90%), oleylamine (Acros, 80-90%), sodium sulfide (Sigma-Aldrich, 99.5%), N-methylformamide (NMFA, VWR, 98%), lithium perchlorate (Sigma-Aldrich, 98%), Polyethylene glycol ($M_W$=6kg.mol$^{-1}$).

**Mercury compounds are highly toxic. Handle them with special care.**

All chemicals are used as received, except oleylamine, which is centrifuged before its usage.

### 1.2. TOPTe precursor

2.54 g of Te powder are mixed in 20 mL of TOP in a three neck flask. The flask is put under vacuum at room temperature for 5 min and then the temperature is raised to 100°C and the degassing is further conducted over the next 20 minutes. The atmosphere is then switched to Ar and the temperature is raised to 275 °C. The solution is stirred until a clear orange solution is obtained. The flask is then cooled down and the color switches to yellow. At room temperature, the flask is degassed again for 10 min. Finally, this solution is transferred to an air free glove box for storage.

## 2. Nanocrystals synthesis

### 2.1. Keuleyan's protocol for MWIR HgTe nanocrystals

Before proposing a new protocol for the synthesis of HgTe CQD, we have investigated the current state of the art synthesis, which has been proposed by Keuleyan *et al*[1] and then improved in reference 2. Briefly, this synthesis relies on the introduction on $HgCl_2$ in oleylamine as the reaction medium. Formation of HgTe starts after the fast injection of TOPTe at a temperature between 60 and 130 °C.

This synthesis is well suited to tune the excitonic feature between 6500 $cm^{-1}$ and 2000 $cm^{-1}$. Size control is made through temperature and time. Higher the temperature and longer the reaction time, larger the particles are, see Figure S 1a. To obtain a narrow size distribution, two critical points have been identified: (i) the introduction of the precursor within a dilute solution and (ii) preventing the cooling of the reaction mixture while the TOPTe is introduced.

Small size particles (< 8 nm) with excitonic feature below 3000 $cm^{-1}$ are typically present a tetrapod shape, see Figure S 1b, while larger particles (8-12 nm) rather have a tetrahedron shape. This change of shape comes with a change of spectrum. Typically, the band edge exciton presents a single component for small particle, while two contributions are clearly observed for larger particles.
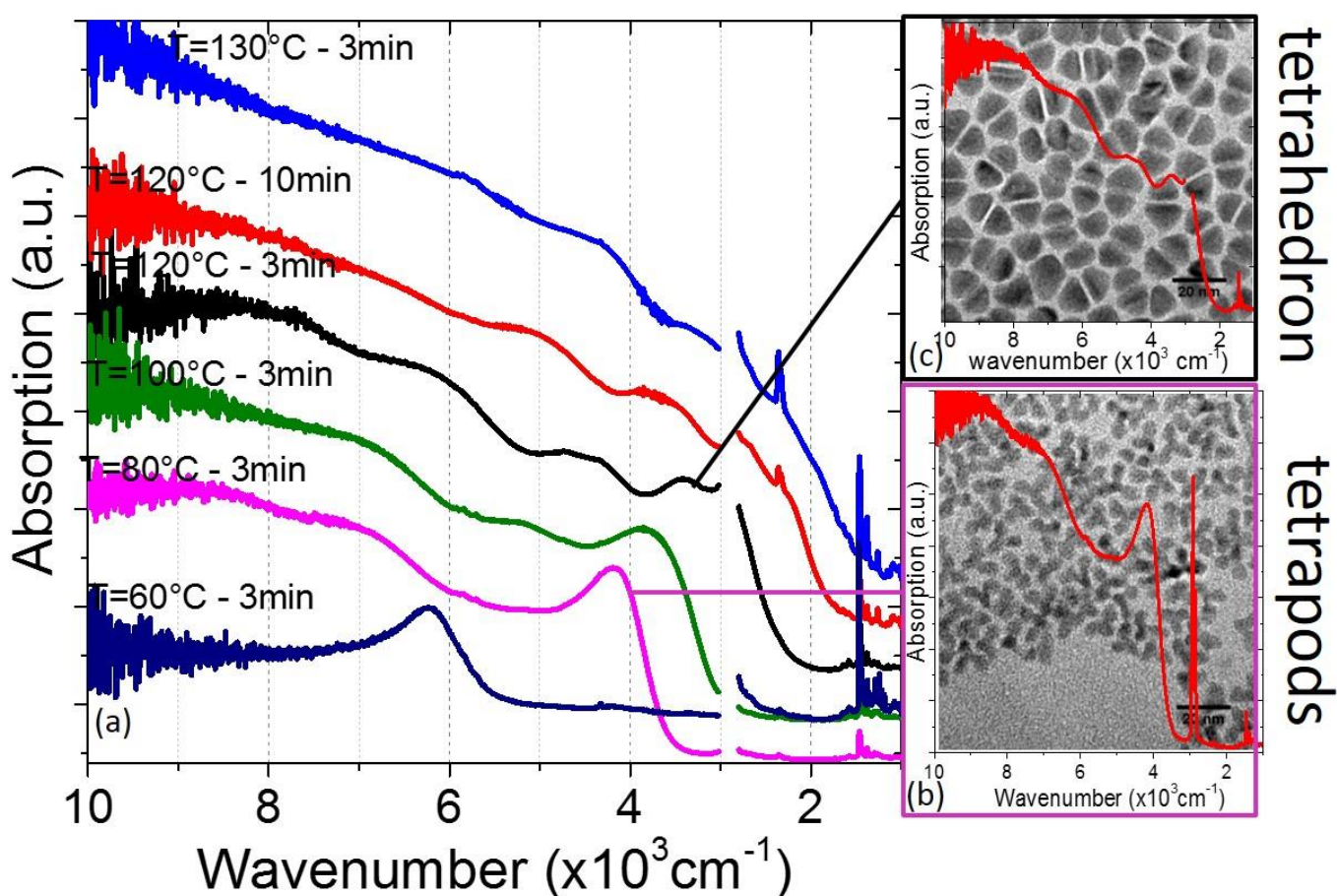


*Figure S 1 (a). Absorption spectra of HgTe synthetized with the Keuleyan procedure[2] for different reaction time and temperature of reaction. Two types of spetra are shown. (b) For small QD, the band edge exciton presents a single component and the TEM image is consistent with tetrapod object. (c) For the largest object the band edge feature is made of at least two component and the TEM analysis reveals tetrahedron shape for these objects.*
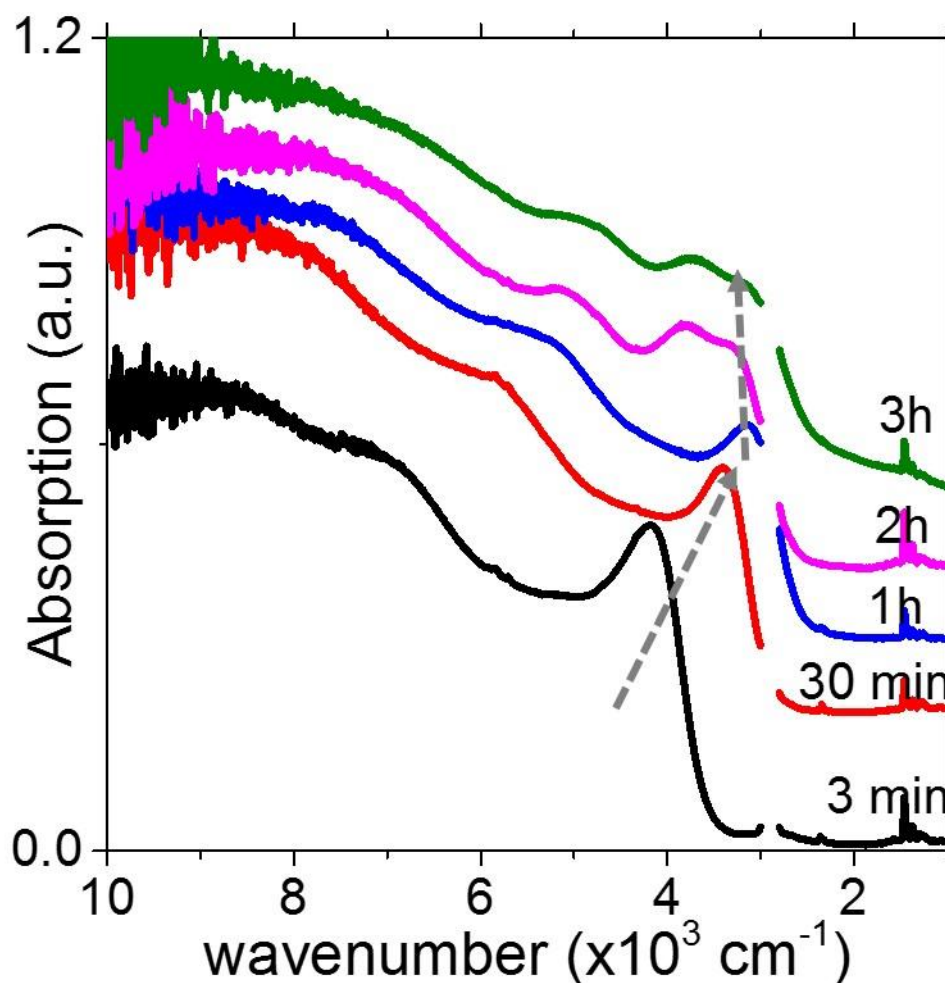
*Figure S 2 Absorption spectra of HgTe synthetized at 80°C with the Keuleyan's procedure[2] for different reaction times*

If the absorption spectra are followed along the reaction time, see Figure S 2, we first see a redshift with time (during the first hour), and then a blue shift (between 1 and 2 hour). To understand this surprising behaviour, transmission electron microscopy is a valuable tool. Again, we see that at early reaction time, the particles are far from spherical shape and come with a tetrapodic shape (see Figure S 3a), compatible with the lattice zinc blende geometry. As a function of time, the length of the arm remains mostly unchanged while they become thicker, see Figure S 3b and c. This increase of thickness continues until the arms start to push each other and the tetrapod breaks apart yielding smaller particles, see Figure S 3d. This separation of different arms is responsible for the blue shift that we observe after 1h, see Figure S 2. The final tetrahedra are actually made of the grown arms of the tetrapods.
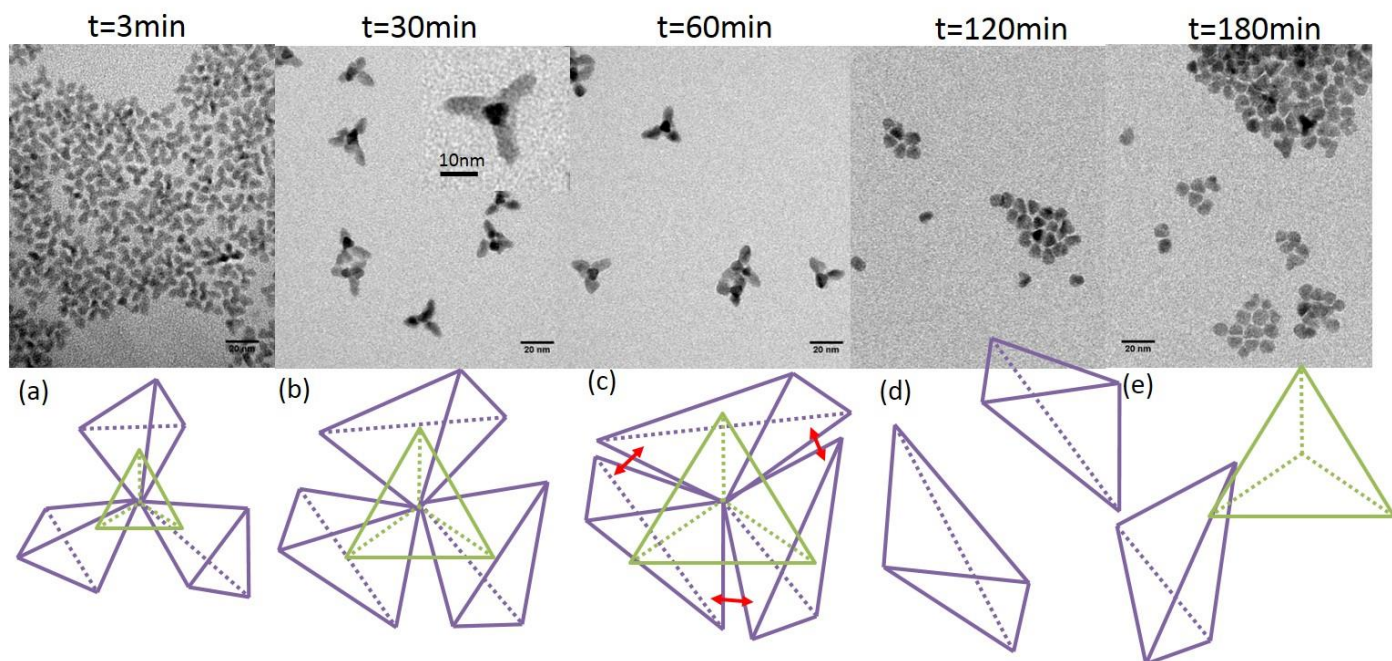
*Figure S 3 TEM images and scheme of the HgTe CQD at different times (a: 3 min, b: 30min, c: 60min, d: 120 min, e:180 min) for a synthesis based on the Keuleyan's protocol[2] and conducted at 80°C. The green tetrahedron is on top of the purple ones*

This tetrahedron shape is responsible for multiple issues. First, the nanocrystals exhibit the least reactive facets {111}, which are poorly favorable for the growth of a shell. Secondly, the flat left facets are extremely favorable to induce self-assembly of tetrahedrons into pairs (see Figure S 4a and b) because of strong ligand interdigitation (distance between nanocrystal is approximately 1.4 nm), see Figure S 4c. The formation of these pairs increase the colloidal radius of the particle and leads to a loss of colloidal stability in spite of the moderate size of the elementary bricks.
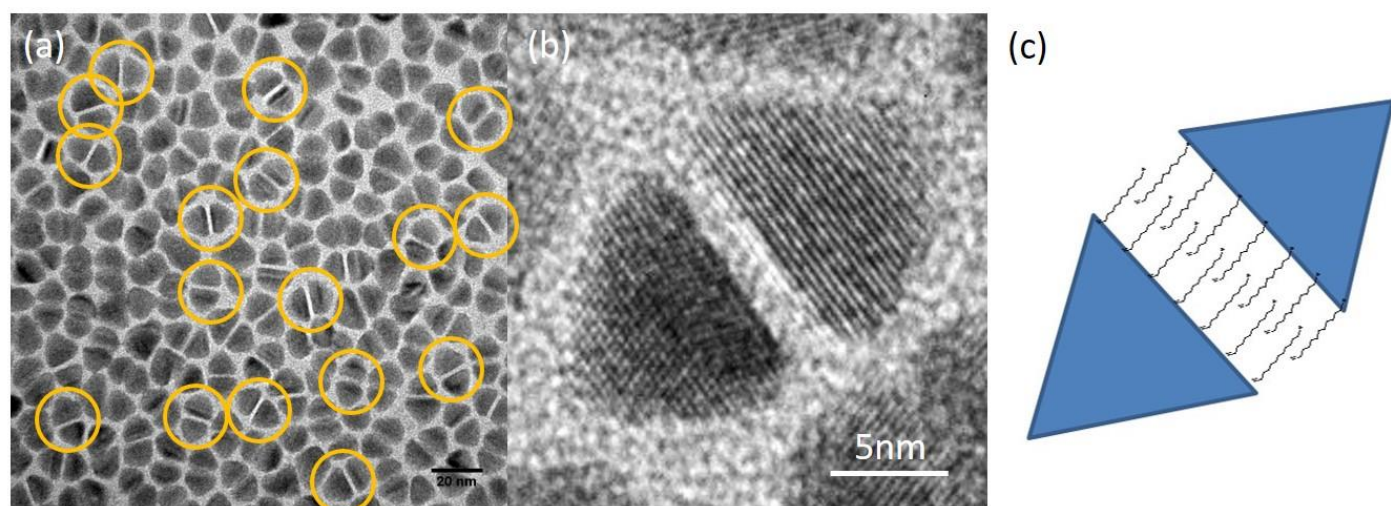


*Figure S 4 TEM (a) and High resolution TEM image (b) of large HgTe tetrahedron obtained through the Keuleyan's synthesis.[2] (c) Scheme of the pair of tetrahedron where we highlight the role play by the ligands in this self assembly process.*

## 2.2. Nanocrystals synthesis

We now propose the following synthesis protocol: 9 mL of oleylamine are placed under vacuum and heated to 120 °C for 1 h. Then, the solution is placed under Ar atmosphere and heated up to the reaction temperature. A second solution is made by mixing 0.1 mmol of $HgX_2$ and 0.1 mL of TOP:Te (1M) in 0.9 mL of oleylamine. The mercury and tellurium solution is quickly injected (within 5 min after mixing) in the hot oleylamine. The solution color quickly turns to dark brown and the reaction is made during 3 min. A solution made of 1 mL of dodecanethiol, 9 mL of toluene and few drops of TOP is quickly added to quench the reaction. 90 mL of ethanol is added to precipitate the nanocrystals from the solution. The colorless supernatant is discarded and the precipitate is redispersed in 3 mL of chloroform and few drops of dodecanethiol. The nanocrystals are washed again with 90 mL of methanol and redispersed in 3 mL of chloroform.

## 2.3. Reactivity of the different halide precursor

To compare the reactivity of three halide precursors of mercury, we follow the absorption at 415 nm, which is a good signature of the total amount of crystallized material, independent of its shape and size, see Figure S 5. In the case of $HgCl_2$, we observe an immediate rise, which is followed by a decay. The latter actually results from the growth of such large particles than they actually lose their colloidal stability and fall at the bottom of the curve. On the other hand, in the case of $HgBr_2$ and $HgI_2$, we observe a continuous rise, meaning that the reaction is still incomplete after 3 hours in the case of $HgI_2$.
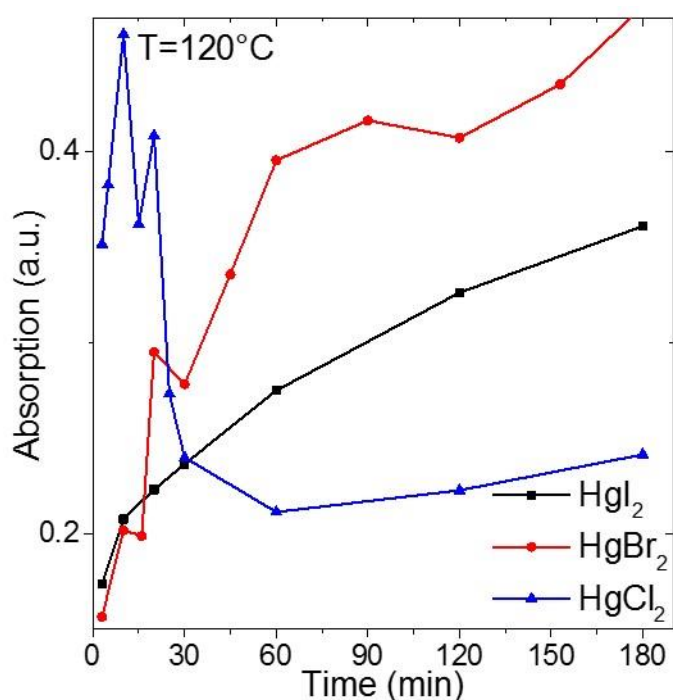


*Figure S 5 Absorption at 415 nm for a synthesis of HgTe CQD conducted at 120°C as a function of the reaction time. The synthesis has been conducted using $HgCl_2$, $HgBr_2$ and $HgI_2$ as mercury precursors.*

## 2.4. Nanocrystal size distribution

Figure S 6 gives the size histogram for HgTe CQD synthetized at different growth conditions and with different Hg precursors. For each population a sample of 200 CQD has been measured. The overall trend is

that higher temperature leads to larger objects and that the halide can be classified as follows in term of final growth size: Cl>Br>I.
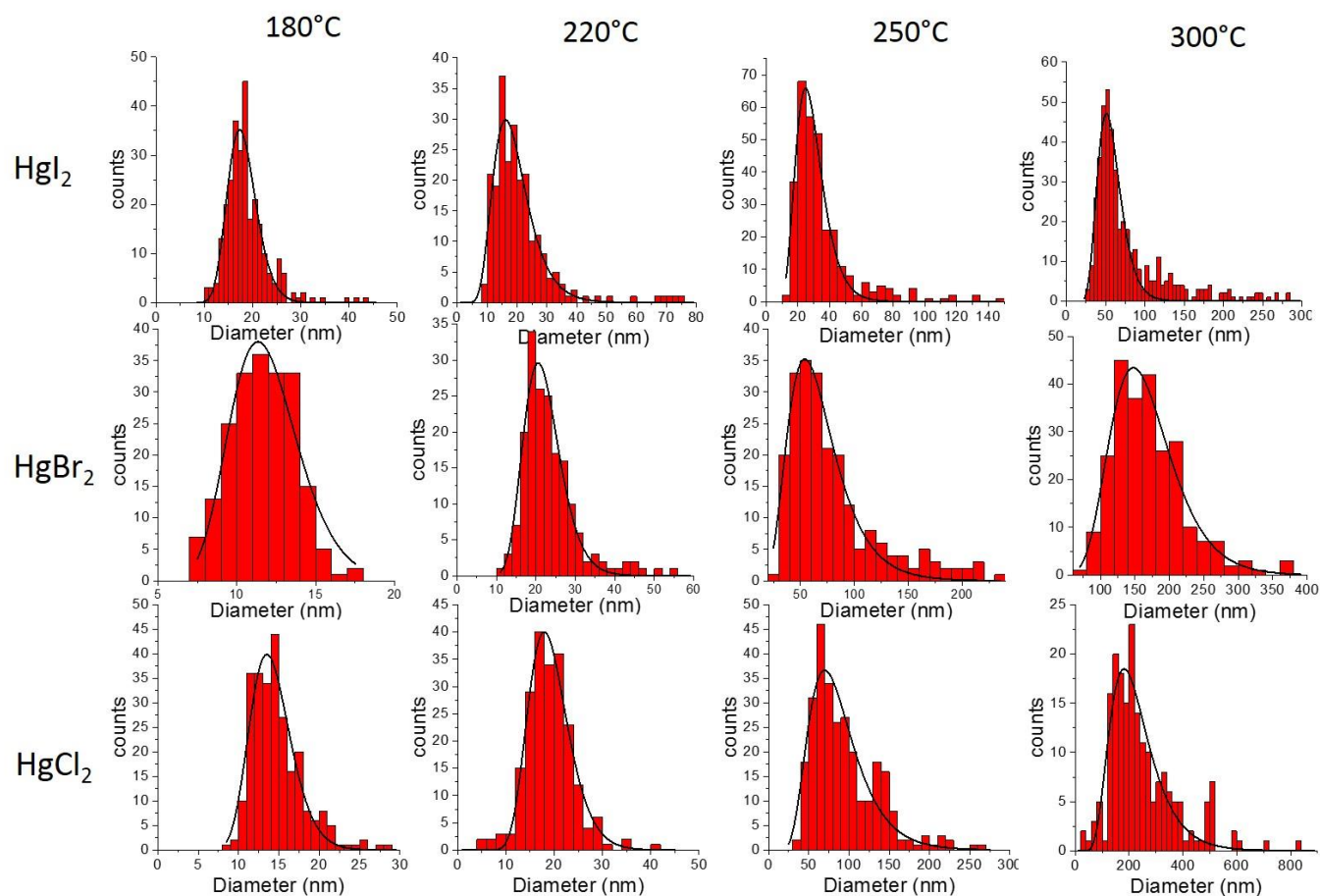


*Figure S 6 Size hitograms of HgTe CQD synthetized with the difefrents halide and for different reaction time. The recation duraction is here set at 3min.*

## 2.5. Nanocrystal size threshold for intraband transition.

It is known that increase of nanocrystal size lead to increase of doping level in narrow band gap quantum dots. Consequently, the intraband/plasmonic feature on the HgTe absorption spectrum appears when nanocrystals reach a given size. As shown in Figure S 7, the intraband transition appears around $1000cm^{-1}$ with a diameter above 15nm and shift to lower energy when nanocrystal size increase. In the case of 5nm nanocrystal, the absorption at low wavenumber is due to the presence of remaining organic ligands.
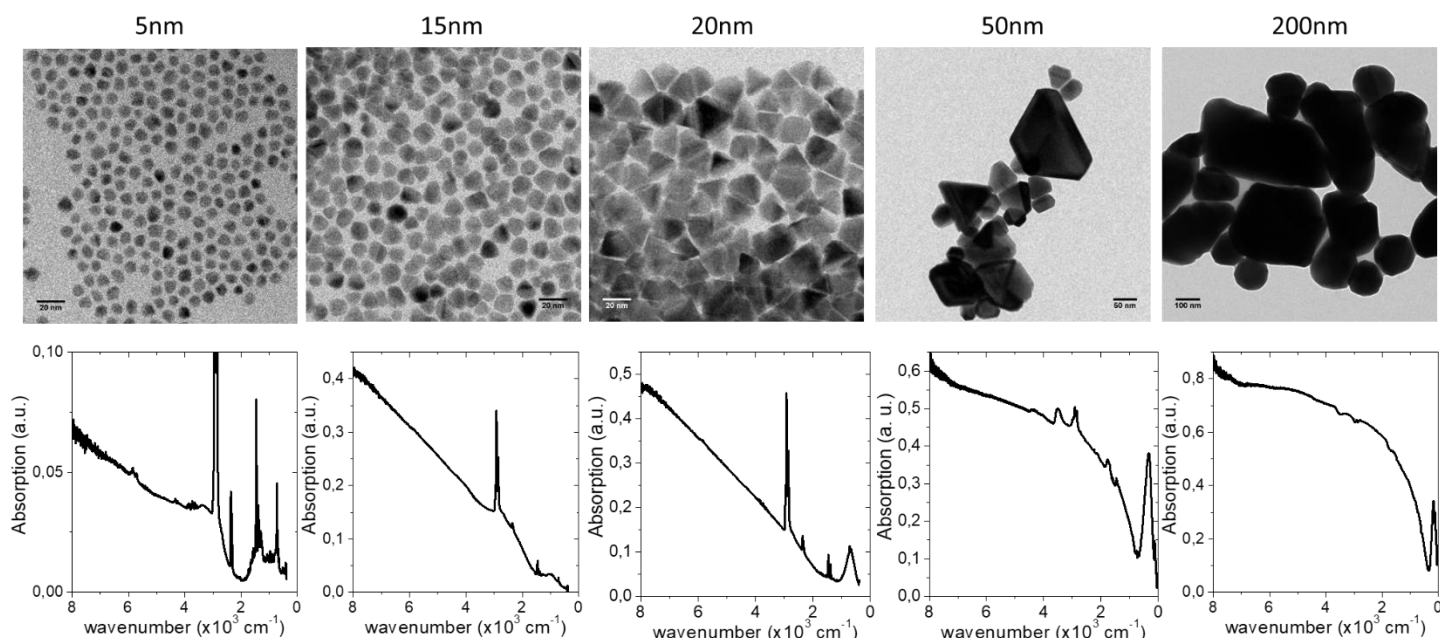
*Figure S 7. TEM pictures of different HgTe nanocrystal size and their corresponding absorption spectra.*

## 2.6. Effect of stoichiometry on the absorption spectra

The long wavelength feature in the absorption spectrum finds its origin in an intraband transition or a plasmonic absorption as it has been proposed for HgS, HgSe[3] and more recently for HgTe[4]. In the case of HgTe, the Te tends to reduce the work function. As a result, the material is not self-doped. Nevertheless, doping can be induced by growing a non-stoichiometric compound. Hg rich condition leads to n-type doping and favors the observation of the long wavelength feature, see Figure S 8
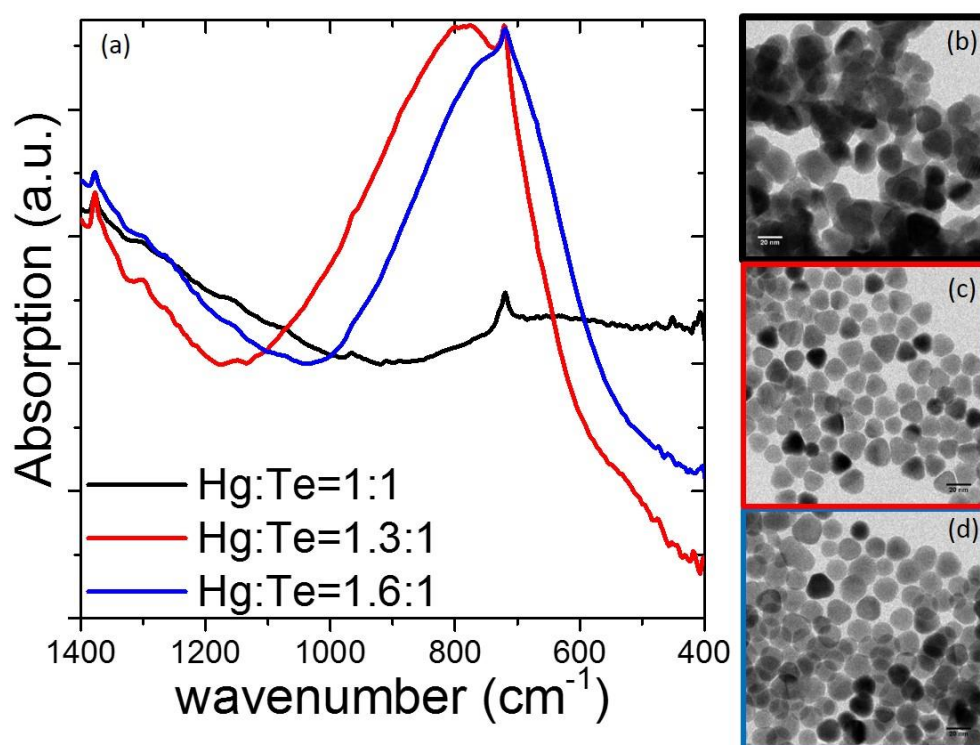
*Figure S 8 Absorption spectra of HgTe CQD obtained while the Hg to Te ratio of precursors is changed from stoichiometric to mercury rich material (a) and repectively the TEM images resulting from synthesis for stoichiometric reaction (b), 30 at% excess of Hg (c) and 60 at% excess of Hg (d).*

## 2.7. Synthesis of HgSe CQD

The protocol has been extended to HgSe. In this case, Se precursor is made of Se powder diluted in oleylamine in presence of $NaBH_4$ to favor the Se reduction. For a typical synthesis:

45 mg of $HgI_2$ or 27 mg of $HgCl_2$ are dissolved in 9 mL of oleylamine and heated to 120°C for 1 h. Then, the solution is placed under Ar atmosphere and heated up to the reaction temperature. A second solution is made by dissolving 1 mmol of Se in 10 mL of oleylamine. 1 mmol of $NaBH_4$ is added to the solution to help dissolution of Se powder at room temperature. 1 mL of this selenium solution is quickly injected in the hot oleylamine containing the mercury precursors. The solution color quickly turns to dark brown and the reaction is made during 3 min. A solution made of 1 mL of dodecanethiol, 9 mL of toluene and few drops of TOP is quickly added to quench the reaction. 90 mL of ethanol is added to precipitate the nanocrystals from the solution. The colorless supernatant is discarded and the precipitate is redispersed with 3 mL of chloroform and few drops of dodecanethiol. The nanocrystals are washed again with 90 mL of methanol and redispersed in 3 mL of chloroform.

At 250°C, the obtained material is very similar to what can be obtained with other methods to grow large size HgSe.[3] The final material is systematically presenting a plasmonic peak (see Figure S 9a and c), consistent with the self-n-doped nature of HgSe even under small size. As for HgTe, chloride leads to larger particles, see Figure S 9b and d.
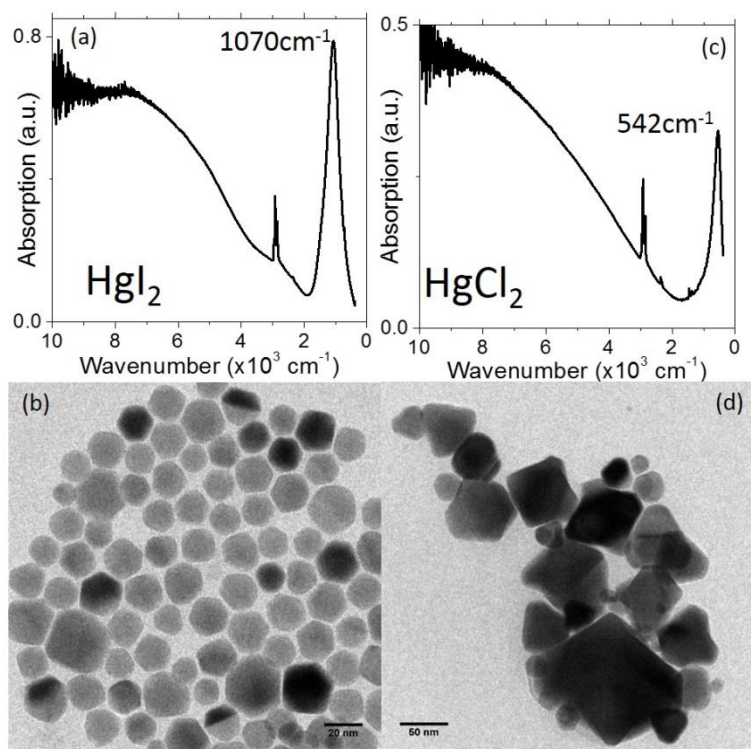


*Figure S 9 (a) absorption spectra of HgSe CQD obtained using $HgI_2$ as precursor. (b) TEM image associated with the material of part (a). (c) absorption spectra of HgSe CQD obtained using $HgCl_2$ as precursor. (d) TEM image associated with the material of part (c).*

## 2.8. Synthesis of HgS CQD

45 mg of HgI$_2$ or 27 mg of HgCl$_2$ are dissolved in 9 mL of oleylamine and heated to 120°C for 1 h. Then, the solution is placed under Ar atmosphere and heated up to the reaction temperature. A second solution is made by dissolving 1 mmol of S in 10 mL of oleylamine at room temperature. 1 mL of this sulfur solution is quickly injected in the hot oleylamine containing the mercury precursors. The solution color quickly turns to dark brown and the reaction is made during 3 min. A solution made of 1 mL of dodecanethiol, 9 mL of toluene and few drops of TOP is quickly added to quench the reaction. 90 mL of ethanol are added to precipitate the nanocrystals from the solution. The colorless supernatant is discarded and the precipitate redispersed within 3 mL of chloroform and few drops of dodecanethiol. The nanocrystals are washed again with 90 mL of methanol and redispersed in 3 mL of chloroform.
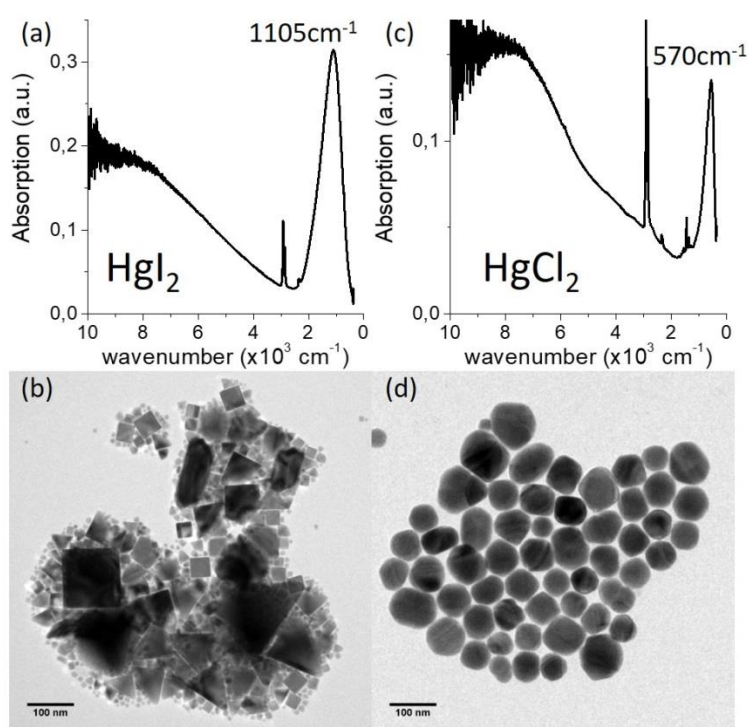


Figure S 10 (a) absorption spectra of HgS CQD obtained using HgI$_2$ as precursor. (b) TEM image associated with the material of part (a). (c) absorption spectra of HgSe CQD obtained using HgCl$_2$ as precursor. (d) TEM image associated with the material of part (c).

## 3. Material characterization

For transmission electron microscopy imaging, we use a dilute solution of nanocrystals in hexane and dropcast on a TEM metallic grid with a carbon support. TEM grid is then degassed overnight under secondary vacuum to remove solvent and small residual organics. The imaging is conducted using a JEOL 2010F microscope operated at 200 kV.

For scanning electron microscopy, we dropcast the solution of CQD onto a doped Si substrate. Imaging is conducted using a FEI Magellan microscope. For imaging, we typically operate the electron beam with a 3 kV bias and a low 6 pA current. Energy dispersive X-ray spectroscopy is conducted in the same instrument using an Oxford probe.

UV visible absorption is conducted using a Shimadzu 3600 spectrometer.

For infrared in the 8000-400 $cm^{-1}$ range, we use a Bruker vertex70 in an ATR configuration. In this case the CQD solution is simply dried on the diamond cell. A Globar source equivalent to a 700°C blackbody is used as source, the beam splitter is made of KBr:Ge and the detector is a DTGS. Spectra are typically acquired between 10 000 $cm^{-1}$ and 380 $cm^{-1}$ with a 4 $cm^{-1}$ resolution and averaging over 32 spectra.

For measurements in the 50-500 $cm^{-1}$ range, we use a Bruker IFS66v. The source is a Globar, the beam splitter is made of 6μm thick film of mylar and the detector is a DTGS with a polyethylene window.

Raman spectroscopy is carried out with a Labram HR800 (Horiba Jobin Yvon) spectrometer equipped with edge filters and coupled with a confocal microscope. The exiting beam was blue 458 nm line from an Argon Laser (Innova 90C-6 from Coherent). The confocal hole, which in our setup also acts as a spectrometer entrance slit, and was fixed at 200 μm. The x100 objective was used to probe the HgTe powder. Spectra are recorded between 50 and 400 $cm^{-1}$ with 1800 lines/mm grating resulting in a resolution of 1 $cm^{-1}$. Spectrometer calibration was set using the 520.5 $cm^{-1}$ band of a Si crystal. The effective laser power at the exit of the objective was between 2 and 4 mW.

### 3.1. Raman spectroscopy

In order to confirm that the observed peak in infrared absorption spectrum at 125cm-1 is resulting from the phonon line, we measure the Raman spectra of a thin film of HgTe CQD. In the 50-400 $cm^{-1}$ range, 4 phonon lines can be observed in Raman: the longitudinal acoustic (LA) phonon at 90.8 $cm^{-1}$, the transverse optic (TO) phonon at 120 $cm^{-1}$, the longitudinal optic (LO) phonon at 140cm$^{-1}$ and a weak peak relative to harmonic of the previous peaks around 260 $cm^{-1}$, see Figure S 11.
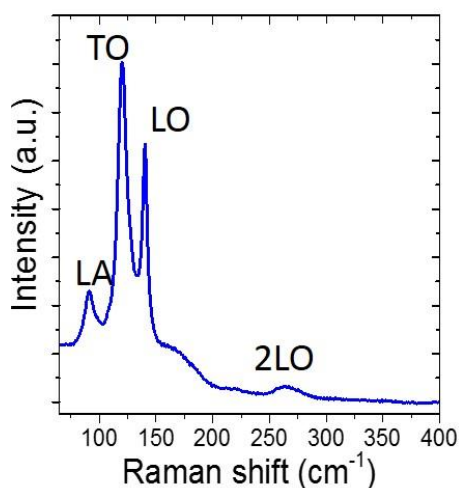
*Figure S 11 Raman spectra for HgTe CQD*

## 4. Transport

### 4.1. Ligand exchange procedure

To prepare thin films of nanoparticles with different capping ligands, we used a liquid phase transfer approach where the CQD end up being $S^{2-}$ capped. To do so, we dissolved $Na_2S$ in NMFA. Some CQD dissolved in hexane are mixed with this solution until a phase transfer occurs. The non-polar supernatant is discarded, before fresh hexane gets added. The polar phase is further cleaned and after decantation, the hexane is removed again. This procedure is repeated for three times. Then, ethanol is added to precipitate the CQD. After centrifugation, the clear supernatant is trashed and the formed pellet redispersed in fresh NMFA.

### 4.2. Electrode fabrication

Electrodes are fabricated using standard optical lithography methods. Briefly, the surface of a $Si/SiO_2$ (400 nm thick) wafer is cleaned by sonication in acetone. The wafer is rinsed with isopropanol and finally cleaned using a $O_2$ plasma. AZ5214 resist is spin coated and baked at 110°C for 90 s. The substrate is exposed under UV through a pattern mask for 2 s. The film is further baked at 125°C for 2 min to invert the resist. Then a 40 s flood exposure is performed. The resist is developed using a bath of AZ726 for 32 s, before being rinsed with pure water. We then deposit a 3 nm Cr layer and a 40 nm gold layer using a thermal evaporator. The lift-off is performed by dipping the film for 1 h in acetone. The electrodes are finally rinsed using isopropanol and dried by air flow. The electrodes are 2 mm long and spaced by 10 μm.

### 4.3. Electrolyte preparation

500 mg of lithium perchlorate ($LiClO_4$) are mixed with 2.3 g of polyethylene glycol (PEG) on a hot plate in an Ar filled glove box at 170°C for 2 h.

### 4.4. Transistor fabrication

The solution of HgTe CQD capped with $S^{2-}$ and dispersed in NMFA is drop casted onto the electrodes on a hot plate at 100 °C under $N_2$ environment. Meanwhile the electrolyte is softened at 100 °C. The melted electrolyte is now clear and is brushed on the CQD film. A copper grid is then deposited on the top of the electrolyte and used as top gate.

### 4.5. Transport measurements

Transport measurements are conducted in air at room temperature. The sample is connected to a dual channel Keithley 2634 which applies drain and gate voltages and measure currents.

## 5. References

(1)  Keuleyan, S.; Lhuillier, E.; Guyot-Sionnest, P. *J. Am. Chem. Soc.* **2011**, *133* (41), 16422.
(2)  Keuleyan, S. E.; Guyot-Sionnest, P.; Delerue, C.; Allan, G. *ACS Nano* **2014**, *8* (8), 8676.
(3)  Lhuillier, E.; Scarafagio, M.; Hease, P.; Nadal, B.; Aubin, H.; Xu, X. Z.; Lequeux, N.; Patriarche, G.; Ithurria, S.; Dubertret, B. *Nano Lett.* **2016**, *16* (2), 1282.
(4)  Shen, G.; Chen, M.; Guyot-Sionnest, P. *J. Phys. Chem. Lett.* **2017**, 2224.